Review of Luminescence Studies on Latent Image Formation in Silver Halide Emulsions

V. M. Belous

Scientific Research Institute of Physics, I. I. Mechnicov State University, Odessa, Ukraine

Certain impurity centers that appear on chemical sensitization of photographic emulsions are shown to induce new photoluminescence (PL) bands of emulsion microcrystals at low temperature, as well as to control photographic properties at room temperature. The nature and function of these centers has been investigated using PL. We found that temperature quenching of some PL bands occurs by an ionic mechanism, specifically neutralization of electrons localized on the recombination center by mobile silver ions in competition with radiative recombination of holes and electrons. Thus, PL and latent image formation appear to be competing processes.

We have also observed the appearance of new PL bands in near infrared (IR) spectral regions as a result of sulfur sensitization and have shown that $(Ag_2S)_n$ clusters of different sizes determine this PL. Further, it has been shown that small clusters are hole traps and that large, mixed $(Ag_2S)_p\, Ag_k^+$ clusters are the centers of photosensitivity. Formation of $(Ag_2S)_n$ and mixed $(Ag_2S)_p\, Ag_k^+$ clusters during sulfur sensitization and Ag_m^0 clusters during reduction sensitization involves silver ions from surface layers of the emulsion microcrystals. This process is accompanied by an increase in structural defects, so that the concentration of uncompensated surface Br_s^- and I_s^- anions increases. These anions are hole traps. Thus, we conclude that during chemical sensitization, hole trap centers are formed but their origin is not necessarily silver or silver sulfide.

Journal of Imaging Science and Technology 41: 85–98 (1997)

Introduction

The increase of photosensitivity of photoemulsions during chemical sensitization is the result of the formation of impurity centers. Different physical and chemical methods such as absorption, electron microscopy, photoelectric methods, photoluminescence (PL), etc., can be used to discover the nature and functions of these centers. Here, we review results obtained by PL on homogeneous emulsion microcrystals.

Experimental Details

In all the studies reviewed in this article we employed silver bromide and silver iodobromide microcrystals in the size range 0.017 to 0.35 μm of various morphologies, all produced by the double-jet method. Standard techniques were employed in all PL studies. Xenon lamp emission, expanded and passed through an optical monochromator, was used for excitation of luminescence. For temperature dependence studies, the samples were heated at a speed of 0.1°/min, and the sample temperature was maintained within ± 0.1° for the duration of the measurement.

Results and Discussion

Influence of Gelatin Adsorption on AgBr(I) and AgBr Microcrystals PL. It is possible to observe PL of silver halide at low temperature (T). Also well known is that the addition of iodide impurities into AgBr leads to the appearance of emission in the green spectral region. It was proposed[1,2] that such emission originates from iodine pair centers. The green PL at 77 K originates by different mechanisms for AgBr(I) single crystals and AgBr(I) microcrystals in gelatin.[3,4] Infrared irradiation of excited AgBr(I) single crystals has been accompanied by a luminescence flash and quenching of the intensity of the PL emission (called IR flash and IR quenching),[5,6] but in the case of AgBr(I) microcrystals only quenching is observed.[3,4] Changes of luminescence properties may be caused by adsorption of gelatin molecules on microcrystals. It is well known that gelatin effectively binds silver ions. Thus, adsorption of gelatin on AgHal microcrystals promotes positive charge formation on the surface of these microcrystals. This redistribution of charge leads to surface band bending that causes a "stretching" of electrons to the surface.

In contrast to AgBr(I) single crystals where luminescence of iodine centers is essentially from bulk and occurs by the Sean-Claesens mechanism,[5] in AgBr(I) emulsion microcrystals, surface centers are responsible for the emission that appears as a result of recombination in donor-acceptor pairs (DAP).[7] This can be described by the following schemes:

$$\begin{aligned} &AgBr(I) + h\nu_{ex} \Rightarrow e + h \\ &I^-I^- + e + h \Rightarrow I^0I^- + e \Rightarrow (I^-)^*I^- \\ &(I^-)^*I^- \Rightarrow I^-I^- + h\nu_{lum}, \end{aligned} \tag{1}$$

$$\begin{aligned} &AgBr(I) + h\nu_{ex} \Rightarrow e + h \\ &(I_s^-I_s^-\cdots, Ag_s^+) + e + h \Rightarrow (I_s^-I_s^0\cdots, Ag_s^0) \Rightarrow \\ &(I_s^-I_s^-\cdots, Ag_s^+) + h\nu_{lum}, \end{aligned} \tag{2}$$

where Scheme 1 refers to single crystals,[5] and Scheme 2 refers to emulsion microcrystals.[7] Here, $I_s^-I_s^-$ is a surface iodine pair center; I^-I^- is a bulk iodine pair center; Ag_s^+ is a surface silver ion; e and h are photoexcited electrons and holes, respectively; and $(I^-)^*$ is excited iodine anion. Accordingly, release of electrons from the recombination

Original manuscript received October 16, 1996.

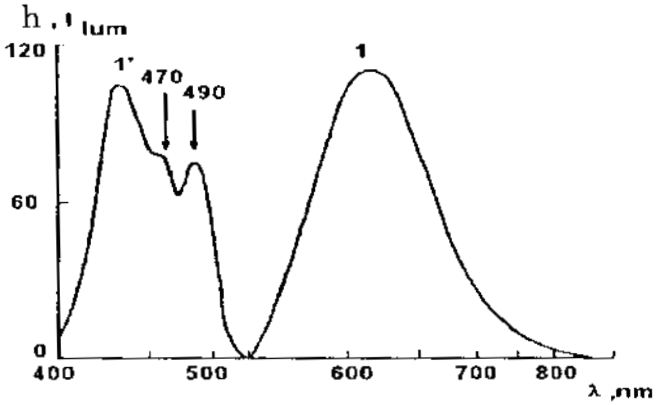

Figure 1. Low-temperature (T = 77 K) phosphorescence spectra (Curve 1) and orange phosphorescence excitation spectra (Curve 1') of AgBr emulsion microcrystals (microcrystal size is 0.24 μm). Intensity values and h are in arbitrary units.

centers (Ag_s^0) under IR radiation should be accompanied by decrease of emission intensity (quenching) without a luminescence flash.

The above mechanisms can be supported by studies of photoluminescence of the silver bromoiodide emulsions formed in polyvinyl alcohol (PVA). In this case, luminescent properties of emulsion microcrystals are the same as for the AgBr(I) single crystals. However, the addition of gelatin on the emulsion formed in PVA sharply decreases intensity of the PL flash in the green stimulated by IR radiation at 77K.[8] The same result is obtained if the concentration of Ag^+ ions adsorbed on the surface of AgBr(I) emulsion microcrystals is raised, e.g., the pAg of an emulsion with homogeneous AgBr(I) microcrystals (1,0 mol% AgI, 0.24-μm-cubic microcrystals) is decreased from 9.0 to 3.0.[8] At T = 77 K, iodine pair centers located on the surface of the cubic AgBr(I) grains ({100} face) yield a PL band with the maximum at λ_{max} = 545 nm, but the same centers located on the surface of the octahedral grains ({111} face) yield a PL band with the maximum at λ_{max} = 560 nm.[2]

Explanations of luminescent properties presented for AgBr(I) emulsion microcrystals can easily be extended to the case of AgBr emulsion microcrystals as well. In this case the orange-band emission (λ_{max} = 600 to 620 nm, T = 77 K) is the result of the donor–acceptor recombination described by the following scheme[7]:

$$\begin{aligned} &AgBr + h\nu_{ex} \Rightarrow e + h(Br_s^- I_s^- \cdots, Ag_s^+) + e + h \\ &\Rightarrow (Br_s^- I_s^0 \cdots, Ag_s^0) \Rightarrow (Br_s^- I_s^- \cdots, Ag_s^+) + h\nu_{lum}, \end{aligned} \tag{3}$$

where Br_s^- is a surface bromide ion located near to the I_s^- ion. Note here that silver bromide always contains adventitious iodide impurities. The results presented in the next sections further confirm the mechanisms of emulsion microcrystal PL suggested above.

Excitation Spectra for AgBr Emulsion Microcrystal Luminescence. The orange photoluminescence (λ_{max} = 600 to 620 nm at T = 77 K) of AgBr emulsion microcrystals can be observed both under continuous excitation and after the excitation ceases. (We follow the usage whereby in the latter case the observed emission is called phosphorescence.) Silver bromide emulsion microcrystal phosphorescence lasted for 0.1 to 1.0 s at T = 77 K, corresponding to mechanisms of DAP radiative recombination. This phosphorescence can be excited within the fundamental absorption band (λ < 460 nm) of AgBr as well as within the excitation regime with λ > 460 nm. Figure 1 (Curve 1') shows the excitation spectra of the orange phosphorescence of AgBr emulsion microcrystals. This plot describes dependence of the quantity $h = I/E$ on the wavelength (λ) of excitation light, where, I is an average intensity of the phosphorescence observed in the time interval between 10^{-3} and 5 10^{-3} s after excitation and E is the total energy of the exciting light at the various wavelengths. In the region with λ > 460 nm the excitation spectrum has[9] two maxima at λ = 470 and 490 nm (Fig. 1, Curve 1'). The maxima in h corresponding to these wavelengths (h_{470} and h_{490}) increase as a result of AgBr emulsion physical ripening when dissolution of small and growth of large microcrystals occur. The data allow us to suggest that centers responsible for excitation bands with λ = 470 and 490 nm in AgBr emulsion microcrystals are centers located on the surface of these microcrystals.

This conclusion can be supported by experimental data obtained from PL studies of AgBr emulsion microcrystals with adsorbed dyes. The following dyes have been used:

Dye **I** is 1,1',3,3'-tetraethyl-5,5'- dicarboetho--xyimidacarbocyanine iodide,

Dye **II** is 1,1',3'-triethyl-3-g-sulfopropyl-5,5'-dietho--xyimidacarbo-cyanine betaine,

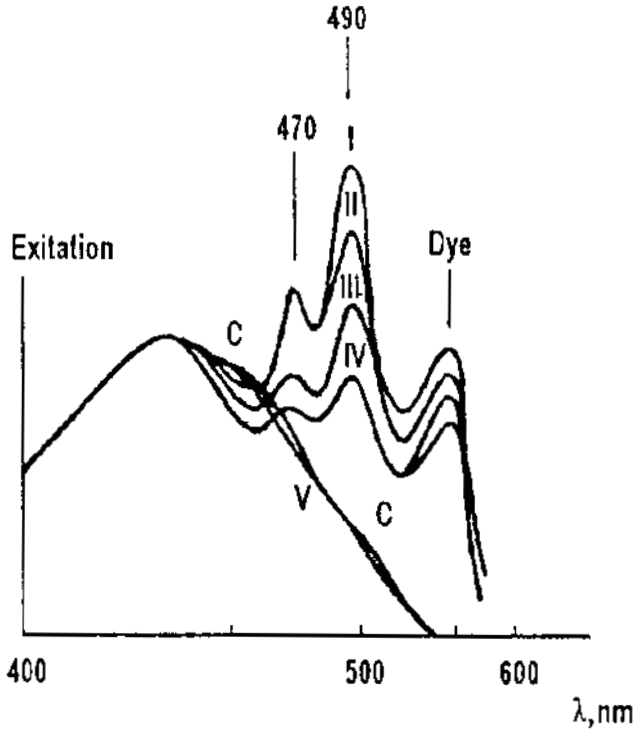

Figure 2. Low temperature (T = 77 K) phosphorescence excitation spectra for Dyes I, II, III, IV, and V adsorbed on the surface of AgBr emulsion microcrystals. Curve C is the excitation spectrum for orange phosphorescence of the emulsion without dye.

TABLE I. Characteristics of Dyes I through V.

Dye	Spectral position of absorption maxims (C_2H_5OH), nm M-band*	H-band	$-E_{1/2\ Red}$, (V)	$E_{1/2\ Ox}$, (V)
I	547	510	1.55	0.67
II	545	520	1.58	0.63
III	543	508	1.60	0.62
IV	545	520	1.53	0.64
V	553*	540	1.05	0.94

*) The M-band maximum for Dye V adsorbed on emulsion microcrystals is λ = 579 nm.

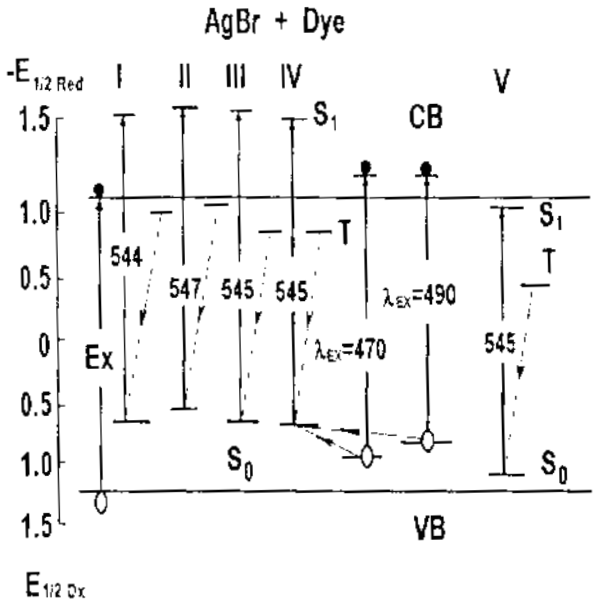

Figure 3. Energy level diagram AgBr with adsorbed Dyes **I**, **II**, **III**, **IV**, and **V**, where: S_0 is the basic singlet level of dye; S_1 and T are excited singlet and triplet levels of dye; numbers at the arrows are the light wavelengths (nm) corresponding to positions of the maxima in the absorption bands.

Dye **III** is 3,3'-di-g-sulfopropyl-1,1'-diethyl-5,5'-dicarboethoxyimida-carbocyanine betaine, sodium salt,
Dye **IV** is 1,1',3,3'-tetraethyl-5,5',6,6'-tetrachlorimida-carbocyanine iodide;
Dye **V** is 3,3',9-triethyl-5,5'-dichlorothiacarbocyanine chloride;

Table I contains the spectral and electrochemical characteristics of these dyes. Reference 10 reports (see Fig. 2) that:

- phosphorescence of adsorbed Dyes **I** through *IV* can be excited both in the dye M-band, and in the bands with λ_{max} = 470 and 490 nm,
- the two bands, λ_{max} 470 and 490 nm, could not be observed in phosphorescence excitation spectra of adsorbed Dye **V**.

These data show the possibility of hole relocalization from ionized centers, responsible for PL excitation spectra at λ_{max} = 470 and 490 nm into the ground state of adsorbed Dyes **I** through **IV**, but not into the ground state of Dye **V**, as represented in Fig. 3. Thus, the following conclusions can be drawn:

1. The centers responsible for the orange PL band are located on the surface of AgBr. According to Scheme 3 we can suppose that bands at λ_{max} = 470 nm (2.63 eV) and 490 nm (2.52 eV) of the excitation spectra of the orange luminescence are caused by the light absorption by surface Br_s^- and I_s^- ions, respectively. In this case the AgBr orange phosphorescence can be explained by the following schemes:

$$(Br_s^- I_s^- \cdots, Ag_s^+) + h\nu(2.63eV) \Rightarrow (Br_s^0 I_s^- \cdots, Ag_s^+) + e$$
$$\Rightarrow (Br_s^- I_s^0 \cdots, Ag_s^0) \Rightarrow (Br_s^- I_s^- \cdots, Ag_s^+) + h\nu_{lum}, \quad (4)$$

$$(Br_s^- I_s^- \cdots, Ag_s^+) + h\nu(2.52eV) \Rightarrow (Br_s^- I_s^0 \cdots, Ag_s^+) + e$$
$$\Rightarrow (Br_s^- I_s^0 \cdots, Ag_s^0) \Rightarrow (Br_s^- I_s^- \cdots, Ag_s^-) + h\nu_{lum}, \quad (5)$$

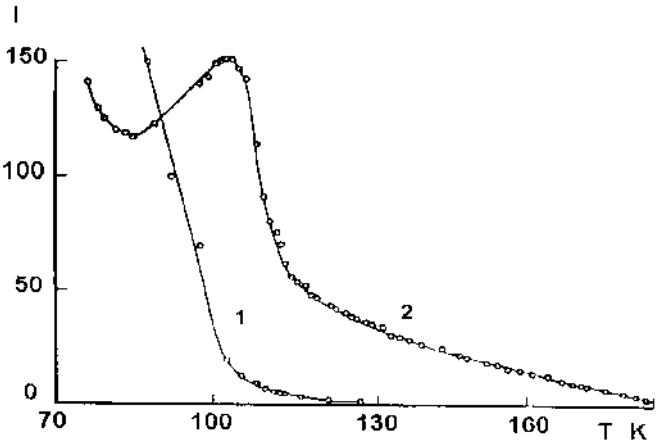

Figure 4. Green luminescence intensity (I) of emulsion AgBr(I) microcrystals as a function of temperature (Curve 1). Curve 2 is the same as Curve 1, but for the case of emulsion grains treated with phenylmercaptotetrazole.

where Br_s^-, I_s^-, Ag_s^+ are closely located surface ions. Scheme 4 includes the possibility of tunneling relocalization of a photohole from a Br_s^0 atom to the nearest I_s^- ion. In accordance with Schemes 3 through 5 AgBr orange emission appears as a result of the radiative recombination of a donor (Ag_s^0)–acceptor ($Br_s^- I_s^0$) pair.

2. The energy level of surface iodine ion is between the ground state of Dyes **I** through **IV** and Dye **V** (see Fig. 3). As follows from data represented in Table I, one can concude that oxidation potential of surface I_s^- anion ($+E_{1/2\ ox}$) is between 0.94 and 0.67 V. Thus the energy level of this anion is located between 0.24 and 0.51 eV above the AgBr valence band.

In addition we want to note that in the case of AgBr(I) microcrystals, a long wavelength threshold of green PL excitation spectra is shifted to λ = 500 nm at T = 4.2 K.

Ionic Mechanism of the Temperature Quenching of the Donor–Acceptor Pair Photoluminescence of AgBr and AgBr(I) Emulsion Microcrystals. The photoluminescence of AgBr(I) and AgBr microcrystals described by Schemes 2 through 4 prevails at $T \geq 77$ K. At lower temperatures one can observe some other PL bands described by different mechanisms (see, for example, Refs. 1, 5, 7, 11–15). Heating of the samples ($T > 77$ K) leads to decrease of the intensity of the luminescent bands (called temperature quenching of emission) described by Schemes 2 through 5 [Fig. 4(a), Curve 1]. The activation energy of temperature quenching is E^a = 0.11 eV,[3,16] which coincides with the activation energy of ionic conductivity due to surface or interstitial silver ions ($Ag_{s,i}^+$). Therefore, we suggested previously[3] that temperature quenching of the orange emission bands from AgBr and green emission bands from AgBr(I) emulation microcrystals occurs according to an ionic mechanism, in other words, by neutralization of the electron localized on the recombination center by mobile silver ion ($Ag_{s,i}^+$) in competition with radiative recombination of this electron with a hole. Raising the temperature causes an increase both in silver ion mobility and in the number of neutralization events that result in the decreased intensity of the above emission bands. This ionic mechanism of emission quenching can be described by the following schemes[7]:

$$\left(Br_s^- I_s^0 \cdots, Ag_s^0\right) + Ag_{s,i}^+ \Rightarrow \left(Br_s^- I_s^0 \cdots, Ag_2^+\right), \quad (6)$$

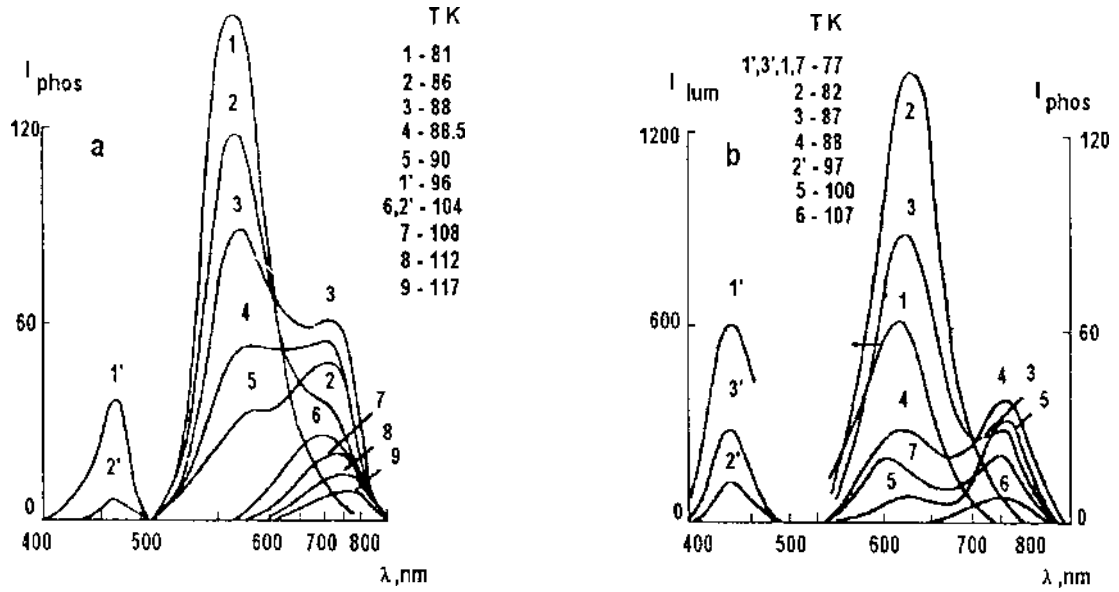

(a) **(b)**

Figure 5. (a) Phosphorescence spectra (1 through 9), excited with 470-nm light, and phosphorescence excitation spectra (1', 2') of AgBr(I) emulsion microcrystals at different temperatures (K). Excitation spectra are measured for phosphorescence bands with λ_{max} = 570 (1') and 700 nm (2'). (b) Luminescence spectra (1), phosphorescence spectra (2 through 7) and excitation spectra (1' through 3') for AgBr emulsion microcrystals at different temperatures. Excitation spectra are measured for the luminescence band with λ_{max} = 600 nm (1') and phosphorescence bands with λ_{max} = 600 (2') and 750 nm (3'). For excitation of phosphorescence (Curves 2 through 7) 430-nm light was used. Curve 7 displays phosphorescence spectra at 77 K for the sample that was cooled to 77 K again after conducting the second round of temperature quenching of luminescence. The luminescence spectra were measured under continuous excitation, and phosphorescence spectra were measured within an interval (1 to 5) $\times 10^{-3}$ s after the excitation light was turned off. Intensity values and the parameter h are shown in arbitrary units.

$$\left(I_s^- I_s^0 \cdots, Ag_s^0\right) + Ag_{s,i}^+ \Rightarrow \left(I_s^- I_s^0 \cdots, Ag_2^+\right), \tag{7}$$

Since the Ag_2^+ center is a deep electron trap, then on continuing excitation of PL further transformation of the silver fragment (see Schemes 6 and 7) into a donor–acceptor pair becomes possible:

$$\begin{aligned}
&\left(Br_s^- I_s^0 \cdots, Ag_2^+\right) + e \Rightarrow \left(Br_s^- I_s^0 \cdots, Ag_2^0\right) + Ag_{s,i}^+ + e \Rightarrow \\
&\Rightarrow \left(Br_s^- I_s^0 \cdots, Ag_3^+\right) + e \Rightarrow \\
&\Rightarrow \left(Br_s^- I_s^0 \cdots, Ag_3^0\right) \Rightarrow \cdots, \Rightarrow \left(Br_s^- I_s^0 \cdots, Ag_n^0\right),
\end{aligned} \tag{8}$$

$$\begin{aligned}
&\left(I_s^- I_s^0 \cdots, Ag_2^+\right) + e \Rightarrow \left(I_s^- I_s^0 \cdots, Ag_2^0\right) + Ag_{s,i}^+ + e \Rightarrow \\
&\Rightarrow \left(I_s^- I_s^0 \cdots, Ag_3^+\right) + e \Rightarrow \\
&\Rightarrow \left(I_s^- I_s^0 \cdots, Ag_3^0\right) \Rightarrow \cdots, \Rightarrow \left(I_s^- I_s^0 \cdots, Ag_n^0\right),
\end{aligned} \tag{9}$$

The ionic mechanism of temperature quenching of luminescence can be proved by the following experimental result. Addition of phenylmercaptotetrazole to the emulsion shifts the quenching regime to higher temperatures[16] [Fig. 4, Curve 2] without changing its activation energy (0.11 eV), as follows from the dependence of ln I on 1/T. We infer that 1-phenyl-2-mercaptotetrazole binds the mobile surface silver ions that participate in the temperature quenching process, as depicted in Schemes 6 through 9.

Creation of new donor–acceptor pairs during temperature quenching of orange photoluminescence from AgBr emulsion microcrystals [e.g., $(Br_s^- I_s^0 \ldots Ag_2^0)$] and green photoluminescence from AgBr(I) emulsion microcrystals [e.g., $(I_s^- I_s^0 \ldots, Ag_2^0)$] results in new luminescence bands. During temperature quenching of the orange PL of AgBr and green PL of AgBr(I), new photoluminescence bands with λ_{max} = 750 and 700 nm, respectively, appeared (see Fig. 5).[17] These bands can be described by the following properties:

1. Peak intensity of these bands increases with activation energy of 0.11 eV in the temperature region where orange PL of AgBr and green PL of AgBr(I) are being quenched,
2. Activation energy for temperature quenching of these bands is also 0.11 eV.

These results correspond to Schemes 8 and 9 and allow us to conclude[17] (Fig. 6) that a luminescence band with λ_{max} = 750 nm in AgBr results from radiative recombination of $(Br_s^- I_s^0 \ldots, Ag_2^0)$, and the luminescence band with λ_{max} = 700 nm in AgBr(I) likewise corresponds to radiative recombination of $(I_s^- I_s^0 \ldots, Ag_2^0)$.

From the results shown in Fig. 6 it is easy to deduce that the energy level of the Ag_2^0 center in the donor-acceptor pair is 0.4-eV deeper than the energy level of Ag_s^0.

According to the above ionic mechanisms of temperature quenching of some luminescence bands, photoluminescence of AgHal and silver cluster formation (including latent image formation) can be seen as two competing processes. In fact, decrease of luminescence intensity, as occurs during temperature quenching, is accompanied by an increase in photographic sensitivity.[16] Note that latent image formation occurs[17]:

1. according to the Mitchell mechanism[18] modified insofar as the silver centers are components of donor-acceptor pairs,
2. as a sequence of exergonic reactions (Schemes 6 through 9), but not as collective processes typical of phase transitions.

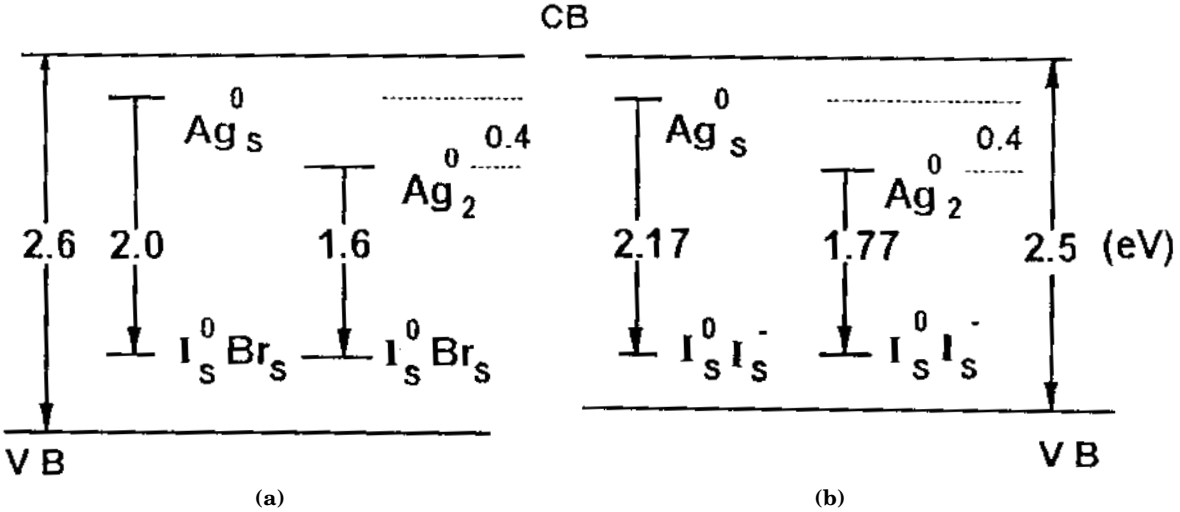

Figure 6. Energy-level diagrams for (a) AgBr and (b) AgBr(I) showing the recombination processes that define different photoluminescence bands: CB, conduction band; VB, valence band.

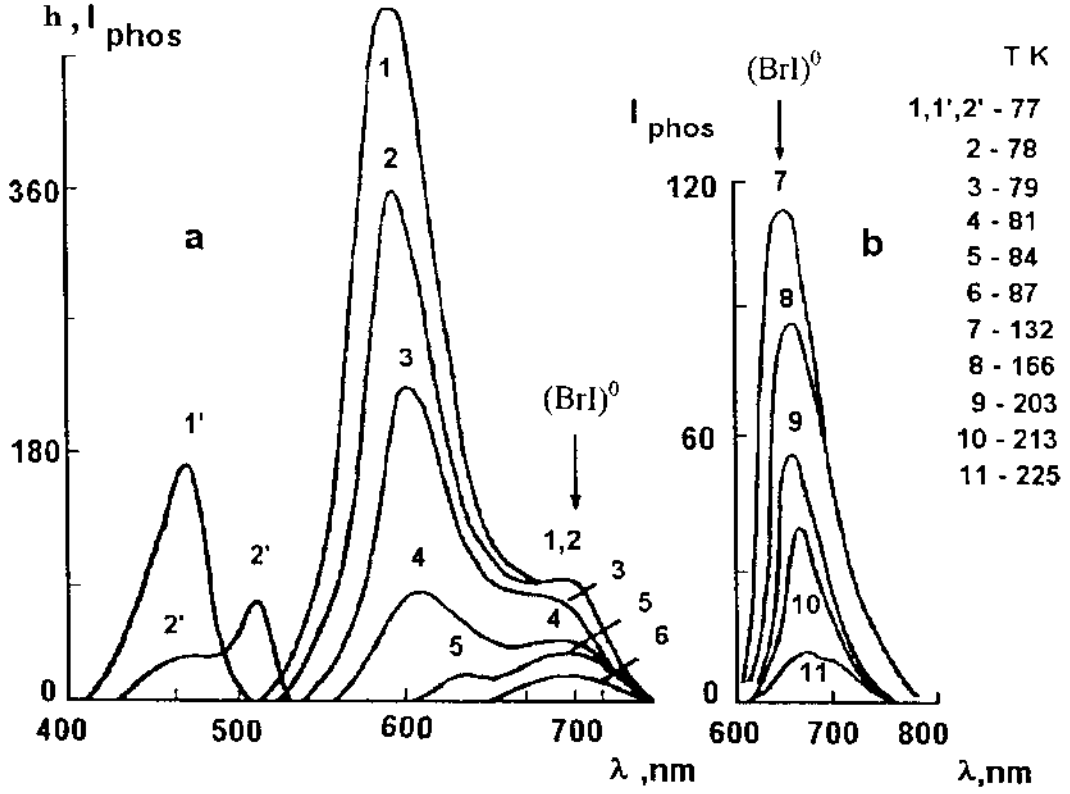

Figure 7. Phosphorescence spectra (1 through 11) and phosphorescence excitation spectra (1', 2') for AgBr emulsion microcrystals at different temperatures (K). Excitation spectra are measured for phosphorescence bands with λ_{max} = 600 (1') and 680 nm (2'). For excitation of phosphorescence at T = 77 to 87 K (Curves 1 through 6) 450-nm light was used, and for excitation of phosphorescence at T = 132 to 225 K (Curves 7 through 11) 520-nm light was used. Intensity values and the parameter h are in arbitrary units.

A fraction of the photoexcited electron population is used for silver cluster formation during temperature quenching of luminescence according to the ionic mechanism. Thus, it is possible for hole accumulation to occur in emulsion microcrystals in that temperature regime. This leads to a higher probability for localization of holes on the (Br_s^- I_s^0) and ($I_s^-I_s^0$) centers that results in creation of $(BrI)^0$ molecules in AgBr and I_2^0 molecules in AgBr(I). These molecules can exhibit new photoluminescence bands.

In fact, we have found new phosphorescence bands with λ_{max} = 680 nm in AgBr and 760 nm in AgBr(I) in the temperature regime for quenching of DAP luminescence. These bands are easily identified if, after measuring the temperature quenching of luminescence, the sample is again cooled to 77 K, for the second round of the investigation. These results are shown in Figs. 7 and 8. The phosphorescence band with λ_{max} = 760 nm also can be observed after adsorption of molecular I_2^0 on the surface of AgBr microcrystals. Therefore, we have inferred that the band with λ_{max} = 760 nm corresponds to phosphorescence of I_2^0 molecules[19,20] and that the band with λ_{max} = 680 nm likewise corresponds to phosphorescence of $(BrI)^0$ molecules. Such phosphorescence can be excited within the fundamental absorption band (λ < 460 nm) of AgBr or AgBr(I) as well as within the excitation regime, λ > 460 nm. In the longer wavelength regime the excitation spectra of I_2^0 molecular phosphorescence has a typical maximum λ = 600 nm ($h\nu$ = 2.05 eV), and in the case of $(BrI)^0$ molecules the typical

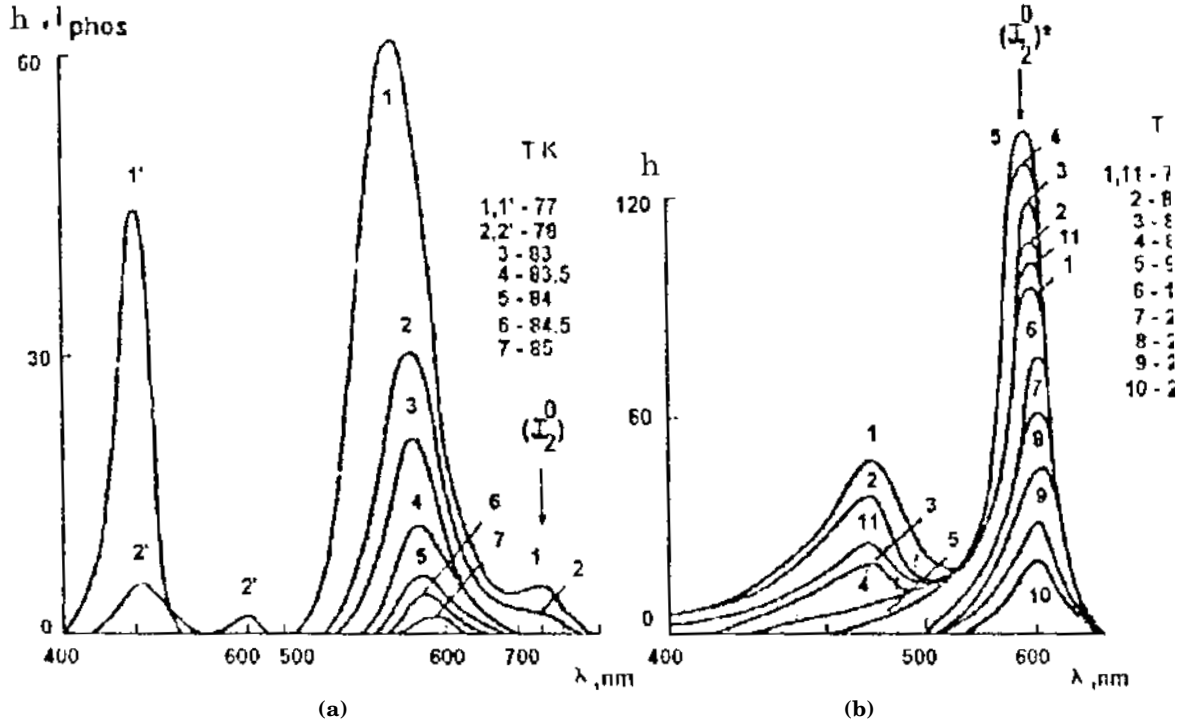

Figure 8. (a) Phosphorescence spectra (1 through 7) excited at 450 nm and excitation spectra (1', 2') for phosphorescence bands with λ_{max} = 570 (1') and 760 nm (2') of AgBr(I) emulsion microcrystals at different temperatures. (b) Excitation spectra (1 thruogh 11) for the phosphorescence band with λ_{max} = 760 nm at different temperatures. Curve 11 displays phosphorescence spectra at 77 K for the sample cooled to 77 K again after conducting the second round of temperature quenching of phosphorescence. Intensity values and the parameter h are in arbitrary units.

maximum is λ = 520 nm ($h\nu$ = 2.38 eV). These two excitation bands correspond to light absorption by I_2^0 and $(BrI)^0$ molecules.

If one uses light with photon energies $h\nu$ = 2.38 eV for excitation of $(BrI)^0$ molecules and $h\nu$ = 2.05 eV for (I_2^0) molecules, their phosphorescence can be observed up to room temperatures (Figs. 7 through 9). Further, if photoexcitation of these molecules occurs by light with λ < 460 nm (the fundamental absorption band of AgBr), the above phosphorescence can be the result of the following processes[20]:

$$\begin{aligned} &AgBr(I)+h\nu_{ex} \Rightarrow e+h \\ &I_2^0+e+h \Rightarrow I_2^- +h \Rightarrow (I_2^0)^* \Rightarrow I_2^0+h\nu_{lum} \end{aligned} \tag{10}$$

or

$$\begin{aligned} &I_2^0 \ldots, Br_s^- (\text{or } I_s^-)+e+h \Rightarrow I_2^- \ldots, Br_s^0 (\text{or } I_s^0)- \\ &\Rightarrow (I_2^0)^* \ldots, Br_s^- (\text{or } I_s^-) \Rightarrow I_2^- \ldots, Br_s^- (\text{or } I_s^-)+h\nu_{lum} \end{aligned} \tag{11}$$

$$\begin{aligned} &AgBr+h\nu_{ex} \Rightarrow e+h, \\ &(BrI)^0+e+h \Rightarrow (BrI)^- +h \Rightarrow (BrI)^* \Rightarrow (BrI)^0+h\nu_{lum} \end{aligned} \tag{12}$$

or

$$\begin{aligned} &(BrI)^0 \ldots, Br_s^- (\text{or } I_s^-)+e+h \Rightarrow (BrI)^- \ldots, Br_s^0 (\text{or } I_s^0) \Rightarrow \\ &-[(BrI)^0]^* \ldots, Br_s^- (\text{or } I_s^-) \Rightarrow (BrI)^0 \ldots, Br_s^- (\text{or } I_s^-)+h\nu_{lum}. \end{aligned} \tag{13}$$

Note that excited molecules $(I_2^0)^*$ and $(BrI)^*$ are the result of the recombination of electrons captured by molecules with a localized hole according to the DAP recombination mechanism. In this case molecular phosphorescence can be observed only at a relatively low temperatures (T < 90 K) and the temperature quenching of this phosphorescence occurs with activation energy of 0.11 eV (Fig. 9). Thus, we have suggested the ionic mechanism of temperature quenching according to the following scheme (by analogy with Scheme 8 or 9):

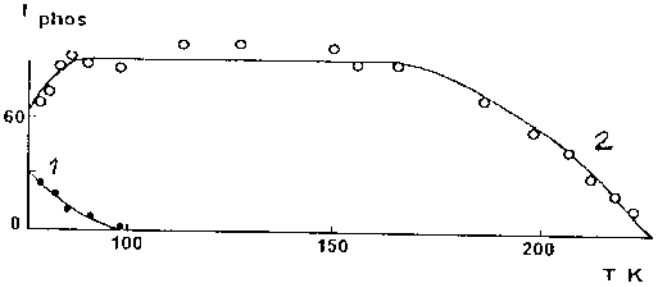

Figure 9. Dependence of the intensity of the phosphorescence band with λ_{max} = 760 nm on temperature for the AgBr(I) emulsion. Light of wavelength (1) λ_{ex} = 470 nm and (2) 600 was used for excitation.

$$I_2^- + Ag_{i,s}^+ \Rightarrow I_2^0 Ag^0 + Ag_{i,s}^+ \Rightarrow I_2^0 Ag_2^+ \ldots, \tag{14}$$

$$(BrI)^- + Ag_{i,s}^+ \Rightarrow (BrI)^0 Ag^0 + Ag_{i,s}^+ \Rightarrow (BrI)^0 Ag_2^+ \ldots, \tag{15}$$

Influence of Irradiation on the Luminescent Properties of AgBr and AgBr(I) Emulsion Microcrystals. The illumination of AgBr and AgBr(I) emulsion microcrystals at low temperature with the light from the fundamental absorption band of silver halide leads not only to (I_2^0) and $(BrI)^0$ molecular phosphorescence, but also to some other results. The PL experiments conducted at T = 4.2 K allowed us to establish the following:

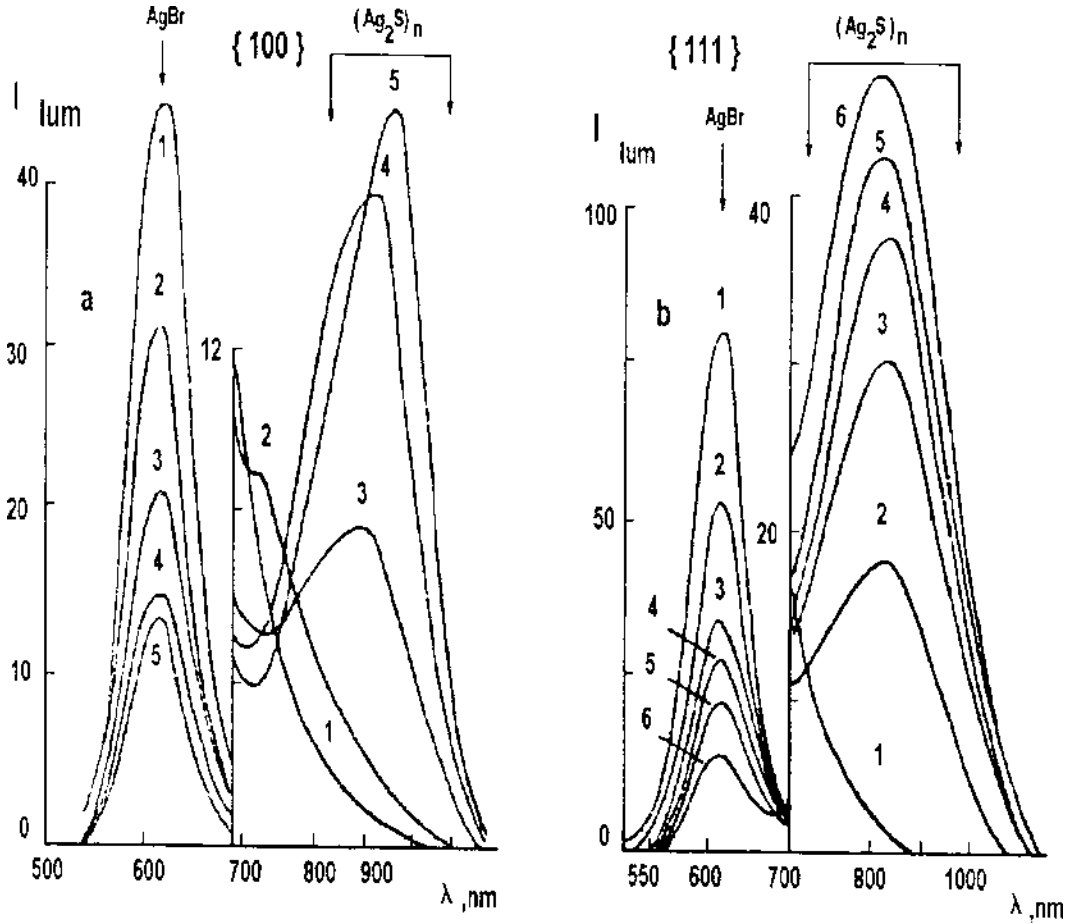

Figure 10. Photoluminescence spectra of photographic AgBr emulsions with (a) 0.35-μm-cubic microcrystals and (b) octahedral microcrystals of the same size for various times (t_2) of digestion with sodium thiosulfate (7.0×10^{-6} mol/g AgBr; pH = 6.0; pAg = 8.7; T = 47°C): (a) Curve 1—t_2 = 0; Curve 2 — 0.5; Curve 3—2; Curve 4—4; Curve 5—6 h; (b) Curve 1—t_2 = 0; Curve 2—0.5; Curve 3—1; Curve 4—2; Curve 5—4; Curve 6—6 hours.

1. Irradiation of AgBr microcrystals stimulates appearance of the photolumi-nescence band with λ_{max} = 550 nm. Maxima at λ = 256, 283, and 450 nm are observed in the excitation spectra of such luminescence.[8] The emission is governed by surface silver atoms that are thermally stable at 4.2 K. The excitation bands appear to be due to electron transitions, specifically $^2S_{1/2} - {}^2D_{5/2}$, $^2S_{1/2} - {}^2D_{3/2}$, and $^2S_{1/2} - {}^2P_{1/2, 3/2}$, of atomic silver. Energy levels of the excited silver atom are in the conduction band of AgBr, and therefore ionization of an excited silver atom is possible, which partially reduces the corresponding PL intensity.
2. After irradiation of AgBr microcrystals, new transitions with λ_{max} = 325 nm ($h\nu$ = 3.80 eV) and 435 nm ($h\nu$ = 2.85 eV) can be observed in the excitation spectra of the various luminescence bands.[20,21] These maxima are associated with light absorption by the I^0 atoms created as a result of hole localization by adventitious iodide ion impurities. The difference between photon energies corresponding to the two maxima of the excitation spectrum is 0.95 eV, which equals the energy of the spin-orbit splitting of the ground state of atomic iodine. These maxima (λ_{max} = 325 and 435 nm) are in the spectral regime of fundamental absorption of AgBr.

Therefore, light absorption by iodine atoms creates free electrons in the conductive band and free holes in the valence band of AgBr. These free carriers further take part in the different recombination processes in silver halides.

Photoluminescence of Sulfur Sensitized Photographic Emulsions. In 1977 we discovered that some new emission bands appear in the near-infrared spectral region (700 nm to 1000 nm) as a result of sulfur sensitization of photographic emulsions comprising AgBr, AgBr(I), and AgCl microcrystals[22–24] (Fig. 10). We established[25] that the chemical nature of the impurity centers that yield IR luminescence in sulfur-sensitized emulsion microcrystals is Ag_2S. Emission bands of the surface silver sulfide centers were recorded at shorter wavelengths (from λ = 700 to 1000 nm) than the photoluminescence of Ag_2S crystals (PL spectrum of Ag_2S crystals exhibits λ_{max} = 1420 nm, and the excitation spectrum of this luminescence has λ_{max} = 1060 nm).[25] The data obtained allowed us to conclude that emission bands in the 700 to 1000-nm spectral regime originate from $(Ag2S)_n$ clusters of different sizes (called quantum-sized centers).[23,25,26] These results were confirmed in subsequent studies.[27,28] The blue shift of the Ag_2S luminescence band with decreasing particle size is now recognized in many other materials.

The dimensional effect on the silver sulfide cluster luminescence can be clearly demonstrated by formation of $(Ag_2S)_n$ clusters in gelatin or polyvinyl alcohol (PVA) solutions (clusters were formed by mixing solutions of $AgNO_3$ and Na_2S).[26,29] High viscosity of gelatin and PVA solutions hinders fast growth and coagulation of silver sulfide particles and promotes appearance of $(Ag_2S)_n$ clusters of different sizes. Clusters formed according to this method have been studied by electron microscopy, which allowed us to determine the size distribution of these clusters.[29]

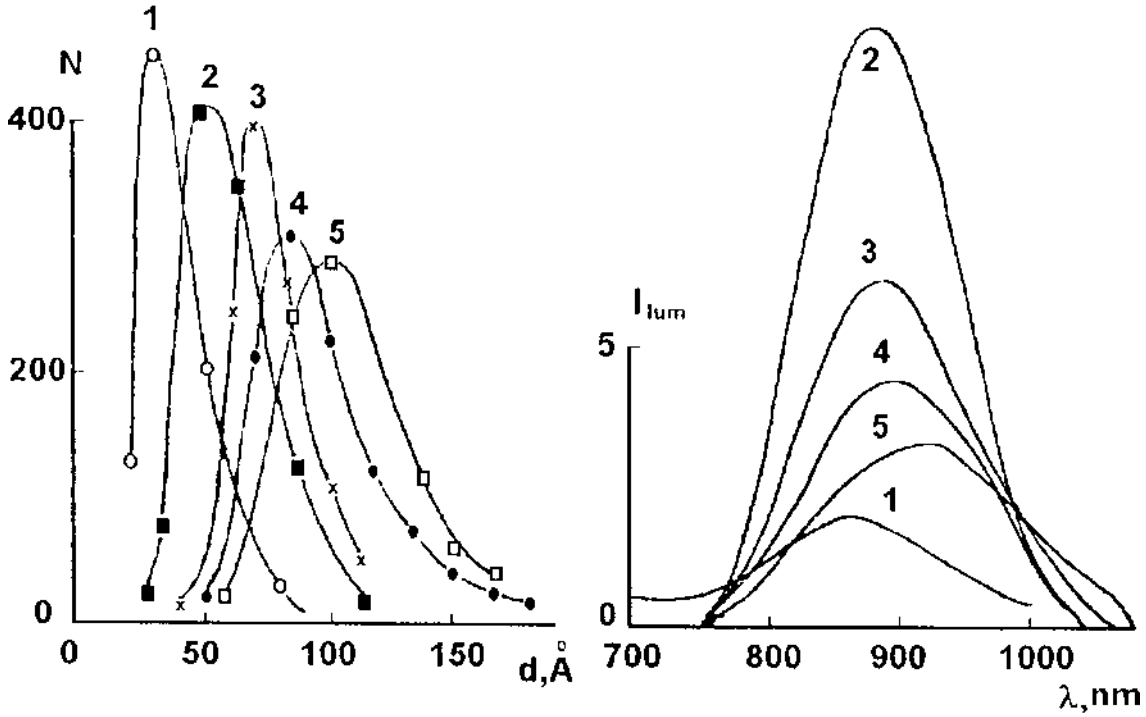

Figure 11. (a) Size distribution and (b) photoluminescence spectra of $(Ag_2S)_n$ clusters obtained by introduction of $AgNO_3$ solutions of various concentrations into the gelatin solution containing Na_2S (2×10^{-3} mol/L): Curve 1 — $[AgNO_3] \times 10^5 = 0.2$ mol/L; Curve 2 — 5.0; Curve 3 — 8.0; Curve 4 — 15.0; Curve 5 — 30.0.

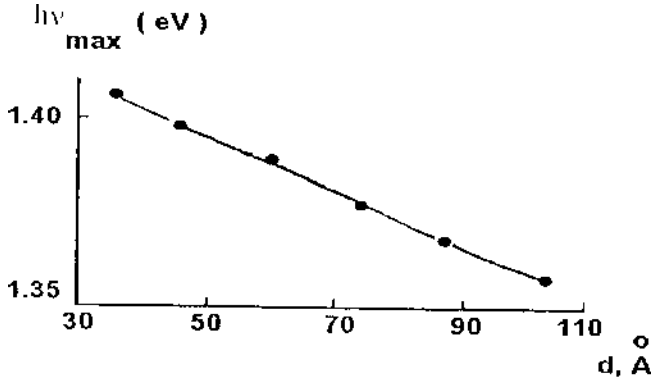

Figure 12. Dependence of the spectral position of the $(Ag_2S)_n$ cluster luminescence band on cluster size.

Accordingly, the linear size (d) of clusters was changed by varying $AgNO_3$ concentration. The distribution of the number of clusters as a function of d for various $AgNO_3$ concentrations (with a constant Na_2S concentration) is shown in Fig. 11(a). The PL spectra for the different $(Ag_2S)_n$ cluster sizes are shown in Fig. 11(b). The dependence of the peak position ($h\nu_{max}$) of $(Ag_2S)_n$ cluster luminescence on cluster size is shown in Fig 12. As can be seen, the larger the cluster size, the smaller $h\nu_{max}$. The luminescence in the regime of λ = 700 to 1000 nm corresponds to clusters with d < 100 Å;[29] $(Ag_2S)_n$ particles larger than 150 Å have PL spectra typical for Ag_2S crystals.[29]

Increasing digestion time (t_2) and/or sensitizer concentration in the AgBr emulsion with cubic microcrystals leads to the shift of $(Ag_2S)_n$ cluster PL band position from 700 to 950 nm [Fig. 10(a)]. This indicates an increase of cluster size during digestion. In the case of octahedral microcrystals, increase of t_2 causes an increase of intensity for the PL band of $(Ag_2S)_n$ clusters without changing spectral position [Fig. 10(b)].[21,23] The data obtained support the conclusion[30] that in the case of cubic grains, silver sulfide deposition occurs according to the autocatalytic law, and in the case of octahedral grains silver sulfide deposition proceeds according to the first-order reaction. The mechanism of Ag_2S formation on the surface of AgBr has been discussed in Refs. 31 and 32.

The luminescence of different size $(Ag_2S)_n$ clusters formed on the surface of silver halide microcrystals can be excited[21,23] by light in the spectral regime between 500 and 680 nm (cluster absorption) as well as in the absorption band of silver halide with λ < 460 nm (Fig. 13). Because energy transfer in silver halide at T > 77 K is solely electron-hole, this result confirms the possibility of localization of the light-induced free carriers on $(Ag_2S)_n$ clusters where cluster emission appears according to the recombination mechanism. Thus, the recombination emission of $(Ag_2S)_n$ clusters is accompanied by a decrease of the intensity of other luminescent bands of AgHal.

If emission of $(Ag_2S)_n$ clusters adsorbed on the silver halide microcrystal surface occurs according to the recombination scheme, then illumination of a sample by IR radiation with λ > 1000 nm should lead to an emission flash from the clusters.[22] We emphasize that the IR flash can be observed only for emission associated with small size clusters and not for large ones (Fig. 14, Curves 1 and 2). As seen in Fig. 14 in the spectral regime of large cluster luminescence (900 to 1200 nm) IR flash was not observed. It is well known that IR-flash luminescence of impurity centers in silver halide occurs only by free-electron recombination with holes localized on the impurity center (see, for example, Refs. 4 and 8). Thus, for $(Ag_2S)_n$ clusters of minimum size the capture cross-section for holes (s_h) is larger than for electron (s_e), so that $(Ag_2S)_n$ clusters of minimum size are better traps for holes. The photoluminescence of $(Ag_2S)_n$ clusters in this case is described by the well-known recombination scheme:

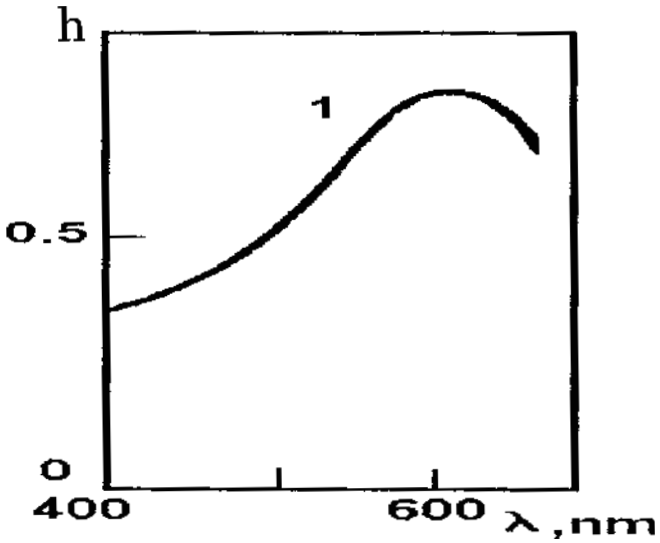

Figure 13. Luminescence excitation spectra of $(Ag_2S)_n$ clusters adsorbed on emulsion AgBr microcrystals; values of h in arbitrary units.

$$(Ag_2S)_n + h + e \Rightarrow (Ag_2S)_n^+ + e \Rightarrow (Ag_2S)_n + h\nu_{lum}. \quad (16)$$

With increasing cluster size, the value of s_e becomes larger than s_h and, thus, the recombination mechanism of the PL changes. Such changes of cluster properties are connected to the fact that increase of cluster size sharply increases the cluster's ability to adsorb mobile (surface or interstitial) silver ions, thus transforming itself into a positively charged $(Ag_2S)_pAg^+$ ($p > n$) cluster that becomes an electron trap. In this case the cluster recombination PL occurs according to the following scheme:[21,33]

$$(Ag_2S)_nAg^+ + e + h \Rightarrow (Ag_2S)_pAg^0 + h \Rightarrow (Ag_2S)_p{}^*Ag^+ \Rightarrow \Rightarrow (Ag_2S)_nAg^+ + h\nu_{lum} \quad (17)$$

or

$$(Ag_2S)_nAg^+ \ldots Br_s^- \text{ (or } I_s^-) + e + h \Rightarrow (Ag_2S)_pAg^0 \ldots, \ldots, Br_s^0 \text{ (or } I_s^0) \Rightarrow \Rightarrow (Ag_2S)_pAg^+ \Rightarrow (Ag_2S)_pAg^+ + h\nu_{lum} \quad (18)$$

where $(Ag_2S)_p^*$ is the excited state of the cluster. In this case, irradiation of the samples in the IR leads to freeing of electrons from recombination centers (Ag^0) and, thus, the luminescence flash cannot be observed.

Addition of reducing agents into the photographic emulsion with silver sulfide clusters of large size adsorbed on the surface of AgBr microcrystals leads to creation of mixed $(Ag_2S)_pAg_m$ or $(Ag_2S)_nAg_m$+ clusters:[21,34]

$$(Ag_2S)_p + Ag_{i,s}^+ + e \Rightarrow (Ag_2S)_pAg^+ + e \Rightarrow (Ag_2S)_pAg^0 + Ag_{i,s}^+ e \Rightarrow \Rightarrow (Ag_2S)_pAg_2^+ + e \Rightarrow (Ag_2S)_pAg_2 \Rightarrow \ldots \Rightarrow (Ag_2S)_pAg_m^+ + e \Rightarrow (Ag_2S)_pAg_m \quad (19)$$

where $Ag_{i,s}^+$ is a mobile surface or interstitial silver ion and e is an electron from the reducing agent.

It was found[34] that the PL of mixed $(Ag_2S)_pAg_m$ or $(Ag_2S)_pAg_m^+$ clusters is observed in the near-IR spectral region, and that their excitation spectrum is red-shifted in comparison with the excitation spectrum of the $(Ag_2S)_p$ cluster emission [Fig. 15(a)]. Destroying the silver fragments in mixed silver sulfide–silver clusters (for example, due to oxidation by gold ions) did not change the emission spectra [Fig. 15(b)], but sharply reduces h in the longer wavelength regime ($\lambda \geq 600$ nm) of the excitation spectrum [Fig. 15(a)].[34] This indicates: (1) that light absorption in the long wavelength regime ($\lambda \geq 600$ nm) of the excitation spectrum was associated with the silver fragment of the mixed cluster; and (2) that the energy transfer from the excited silver fragment to $(Ag_2S)_p$ was possible. In this case the luminescence of the $(Ag_2S)_pAg_m^+$ cluster can arise by the following schemes:

$$(Ag_2S)_p + Ag_m^+ + e + h \Rightarrow (Ag_2S)_pAg_m{}^0 + h \Rightarrow (Ag_2S)_pAg_p{}^*Ag_m{}^+ \Rightarrow \Rightarrow (Ag_2S)_pAg_m^+ + h\nu_{lum} \quad (20)$$

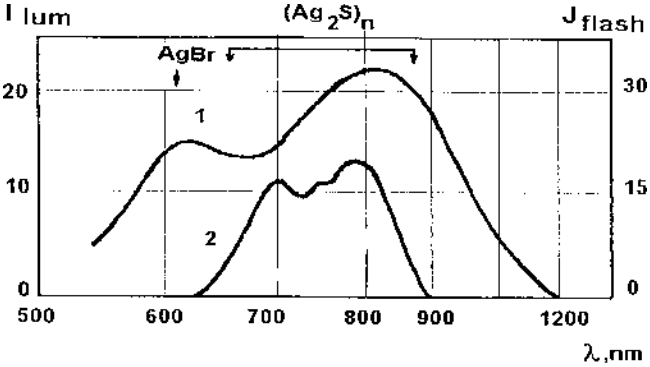

Figure 14. (1) Luminescence spectra and (2) flash luminescence spectra of sulfur-sensitized AgBr emulsion. Intensity values are in arbitrary units.

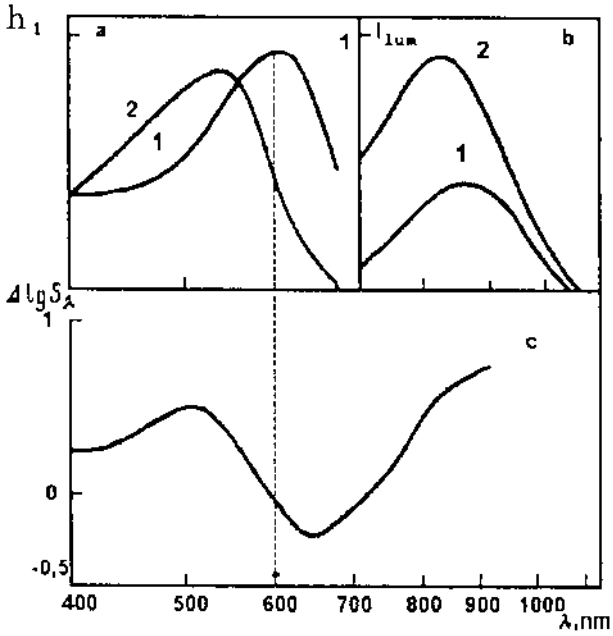

Figure 15. (a) Photoluminescence excitation spectra and (b) photoluminescence spectra of sulfur-sensitized AgBr emulsion (1) before and (2) after treatment in a solution of $KAu(CNS)_2$ (5.1×10^{-6} mol/L) for 30 min (size of cubic AgBr microcrystals is 0.24 μm; fog density, $D_0 = 0.7$). (c) Change of the impurity sensitivity spectra of sulfur-sensitized AgBr emulsion after treatment in the $KAu(CNS)_2$ solution as above. Intensity values and values of the parameter h are in arbitrary units.

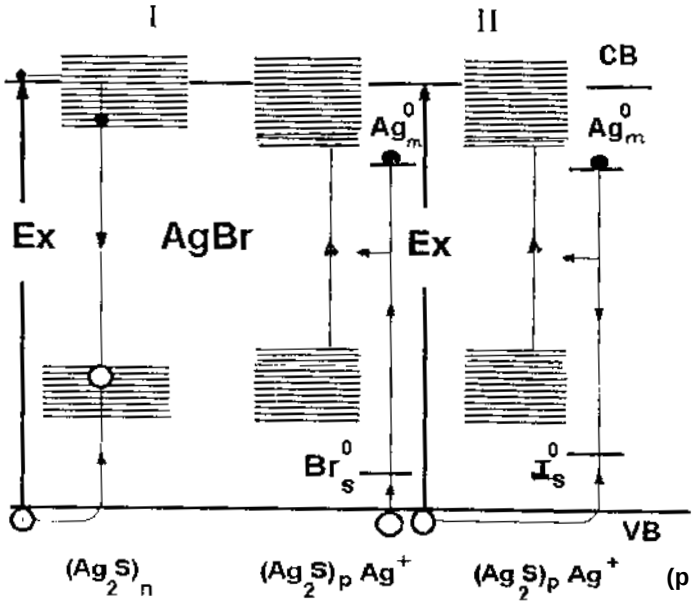

Figure 16. Energy-level diagram for AgBr with adsorbed $(Ag_2S)_n$ (I) and $(Ag_2S)_pAg_m^+$ (II) as inferred from study of the clusters' luminescence. For the excitation of luminescence light absorbed by AgBr was used. The horizontal arrows schematically illustrate the process of the energy transfer to the $(Ag_2S)_p$ cluster.

+

or

$$(Ag_2S)_pAg_m^+ ..., Br_s^- (or\ I_s^-) + e + h \Rightarrow (Ag_2S)_pAg_m^0 ..., ..., Br_s^0 (or\ I_s^0) \Rightarrow$$
$$\Rightarrow (Ag_2S)_p{}^*Ag_m^+ \Rightarrow (Ag_2S)_pAg_m^+ + h\nu_{lum} \quad (21)$$

or

$$(Ag_2S)_pAg_m^+ + h\nu_{ex}(2.0\ eV) \Rightarrow (Ag_2S)_i(Ag_m^+)^* \Rightarrow$$
$$\Rightarrow (Ag_2S)_pAg_m^+ + e \Rightarrow (Ag_2S)_pAg_m^+$$
$$\Rightarrow (Ag_2S)_pAg_m^+ + h\nu_{lum} \quad (22)$$

where $(Ag_m^+)^*$ is an excited state of the silver fragment. Figure 16 shows the processes described by Schemes 16, 18, and 21.

The luminescence of $(Ag_2S)_pAg_m^+$ clusters (m = 1, 2,...), whose appearance may be described by Schemes 17, 18, 20, and 21, can be observed only at low temperature (T < 120 K). The temperature quenching of this luminescence is caused by the ionic mechanism (by analogy with the mechanisms described by Schemes 6 through 9). If, however, one uses light absorbed by the cluster for excitation, cluster luminescence can be observed up to room temperature.[25]

Compare experimental results with theoretical calculations of Ershov, Ionova, and Kiseleva[35] presented in Table II. They have calculated the energy gap (ΔE) between occupied and empty energy levels of the silver clusters of various sizes and charges. As seen from the data in Table II, for the cluster Ag_4^+, ΔE equals 1.9 to 2.0 eV. Thus, such a cluster should absorb in the spectral regime of λ = 600 nm.

Note that the presence of the excitation band with λ_{max} = 600 nm in the excitation spectra for the luminescence of the mixed clusters correlates with the appearance of photographic fog.[34] Both the fog density and this excitation band disappear after destroying the silver fragment of the mixed cluster[34] [Fig. 15(a) and Fig. 17] . On the other hand, addition of the reducing agent (for example, thiourea dioxide) into photographic emulsions with silver sulfide clusters of large size adsorbed on the surface of AgBr microcrystals leads to increase of both fog density and intensity of the excitation band with λ = 600 nm.[21,34] Thus, we have concluded that fog centers are mixed silver–sulfide silver clusters $(Ag_2S)_pAg_m^+$ (it is possible that m = 4, see Table II) and that developing capacity depends on the size of the silver fragment.[21,34] The silver fragment of fog centers is a result of the reducing properties of gelatin molecules. Mixed $(Ag_2S)_pAg_m^+$ clusters are created in the later phases of sulfur sensitization, when large silver sulfide clusters already have been formed. Furthermore, destruction of the silver fragment is accompanied by a

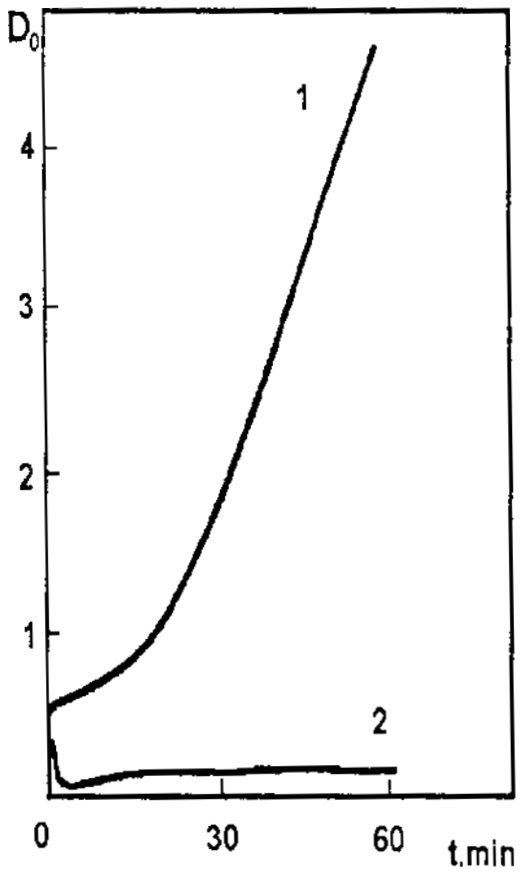

Figure 17. The fog density (D_0) as a function of digestion time period, t_2, of the AgBr emulsion (1) before and (2) after treatment in the $KAu(CNS)_2$ solution (conditions as for Fig. 15).

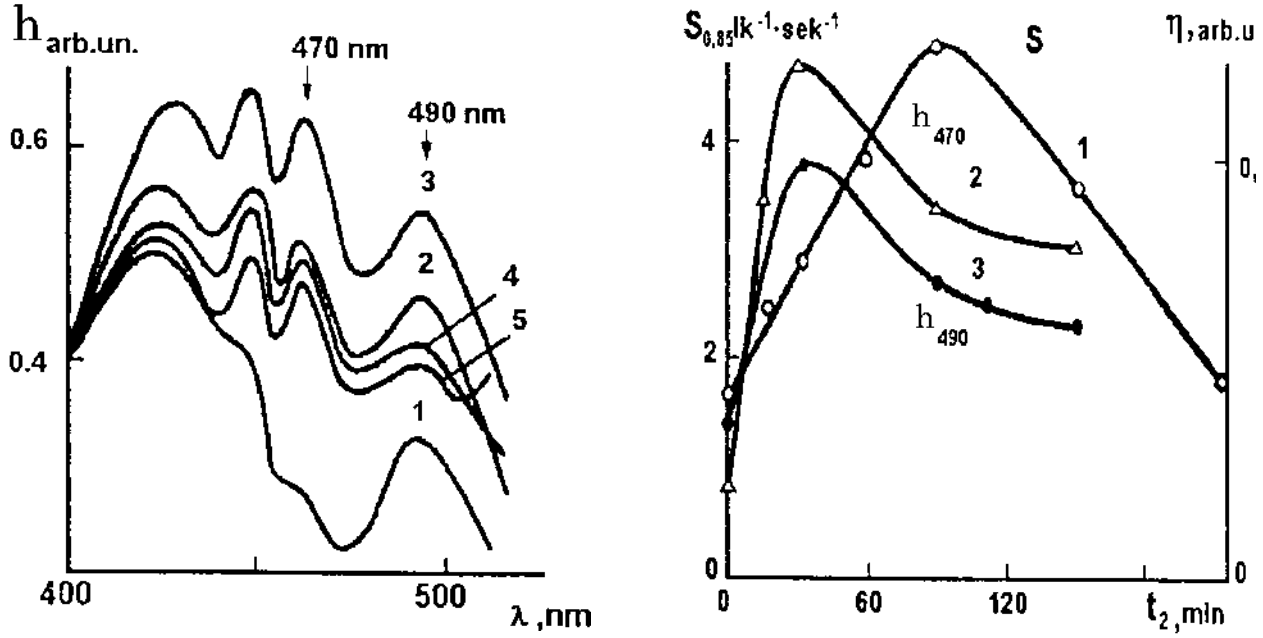

Figure 18. (a) Orange photoluminescence excitation spectra for the samples of the sulfur-sensitized 0.21-μm-cubic AgBr emulsion with different digestion times (t_2, min): 1 — t_2 = 0; 2 —15; 3 — 30; 4 — 90; 5 — 150. Spectra normalized at λ = 400 nm. (b) Dependence of (1) photographic speed, (2) h_{470}, and (3) h_{490} on t_2; values of h_{470} and h_{490} are in arbitrary units. (Digestion conditions for these experiments: $[Na_2S_2O_3] = 2.2 \times 10^{-3}$ mol/mol AgBr; pH = 6.0; pAg = 8.7; T = 47°C).

TABLE II. Energy Gap Value (eV) Dependence on Size and Charge of Silver Clusters.

n	m = 0	m = +1	m = +2	m = +3	m = +4
2	2.6 – 3.0	3.1 – 3.4			
3	1.7	1.3 – 1.8			
	2.1 _ 2.3	1.3 – 1.8			
configuration					
4	1.8 – 2.0	1.9 – 2.1	3.2 – 3.7		
					
configuration					
8	2.0 – 2.3	2.0 – 2.5	2.1 – 2.6	2.1 – 2.6	2.5 – 2.8
14	0.418	0.427	0.386	0.352	

decrease in the impurity-based photosensitivity for wavelengths λ ≥ 600 nm [Fig. 15(c)].[34]

These data allow us to draw the following conclusions:

1. The silver sulfide molecules and small silver sulfide clusters $(Ag_2S)_n$, appearing as a result of sulfur sensitization, are hole traps. This corresponds to Mitchell's conclusions (see, for example, Ref. 36) that silver sulfide centers have hole-acceptor properties. The appearance of such centers does not lead to increase of photographic sensitivity. Therefore, not all silver–sulfide centers are centers of photosensitivity, as emphasized by Chibisov.[37]
2. Sensitivity centers are obviously $(Ag_2S)_p$ clusters capable of adsorbing silver ions, and, thereby, gaining a positive charge. As discussed above, the developing capacity of the $(Ag_2S)_pAg_m^+$ mixed cluster depends on the size of the fragment Ag_m^+ (see also Ref. 38). If the size of the silver fragment is less than some critical size (Ag_m^+), the mixed $(Ag_2S)_pAg_k^+$ clusters (with $k < m$) will be the photosensitivity centers. Thus, the following scheme describes the evolution of photosensitivity centers during sulfur sensitization:

$$(Ag_2S)_pAg^+ \Rightarrow (Ag_2S)_pAg_2^+ \Rightarrow \ldots, \Rightarrow (Ag_2S)_pAg_k^+ \text{ or } (Ag_2S)_pAg_k^0. \quad (23)$$

The increase of the silver fragment size during sulfur sensitization correlates with the accumulation of silver on the surface of the emulsion microcrystals, which can be detected by a microanalytical chemical method.[37]

3. Latent image formation in sulfur–sensitized emulsions is described accordingly by the scheme[7,21]:

$$\begin{aligned}(Ag_2S)_pAg_k^+ + e &\Rightarrow (Ag_2S)_pAg^0{}_k + Ag_{i,s}^+ + e \\ &\Rightarrow (Ag_2S)_pAg_{k+1}^+ + e \Rightarrow (Ag_2S)_pAg_{k+1}{}^0 + Ag_{i,s}^+ + e \\ &\Rightarrow (Ag_2S)_pAg_{k+2}^+ + e \ldots, \Rightarrow (Ag_2S)_pAg_m^+, \quad (24)\end{aligned}$$

where k = 1, 2, ..., < m.

Silver sulfide cluster formation is not the only result of sulfur sensitization of photographic emulsions. Sulfur sensitization also leads to the following:

1. At the initial stage of sulfur sensitization the increase of h_{470} and h_{490} in the excitation spectra of the orange emission of AgBr emulsion microcrystals has been observed[39–41] [Fig. 18(a)]. The quantities h_{470} and h_{490} as functions of t_2 reach[40] their maxima earlier than photographic speed S [Fig. 18(b)].
2. Sulfur sensitization reduces the intensity of the PL band associated with adventitious iodine anion

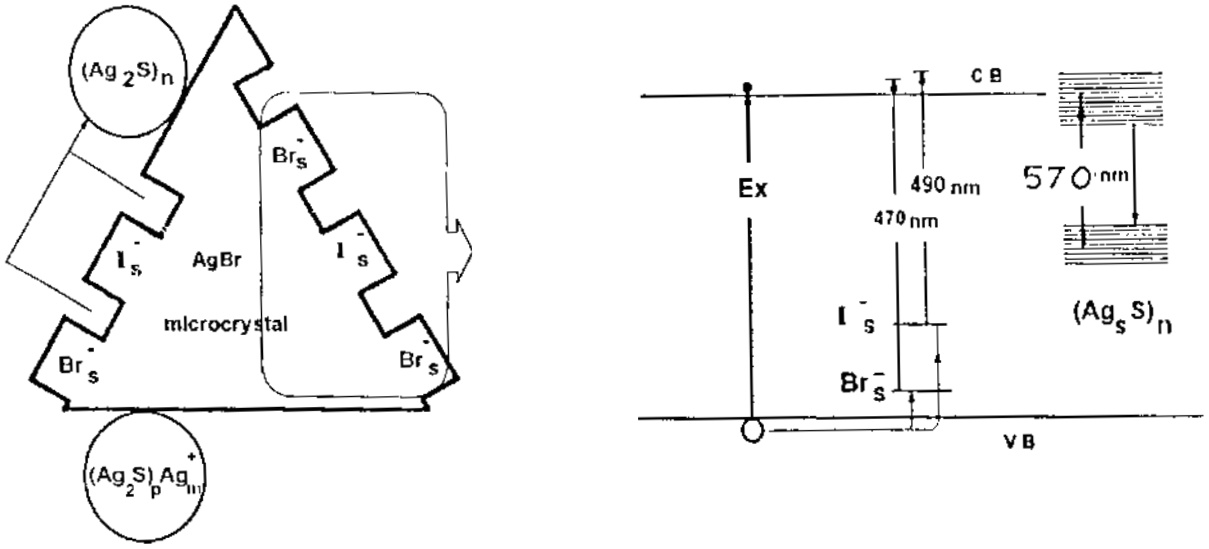

Figure 19. (a) Schematic diagram for the generation of silver sulfide clusters on the surface of a sulfur-sensitized AgBr microcrystal by reaction with surface silver ions. (b) The energy levels of some impurity centers that appear in conjunction with sulfur sensitization of AgBr emulsion grains.

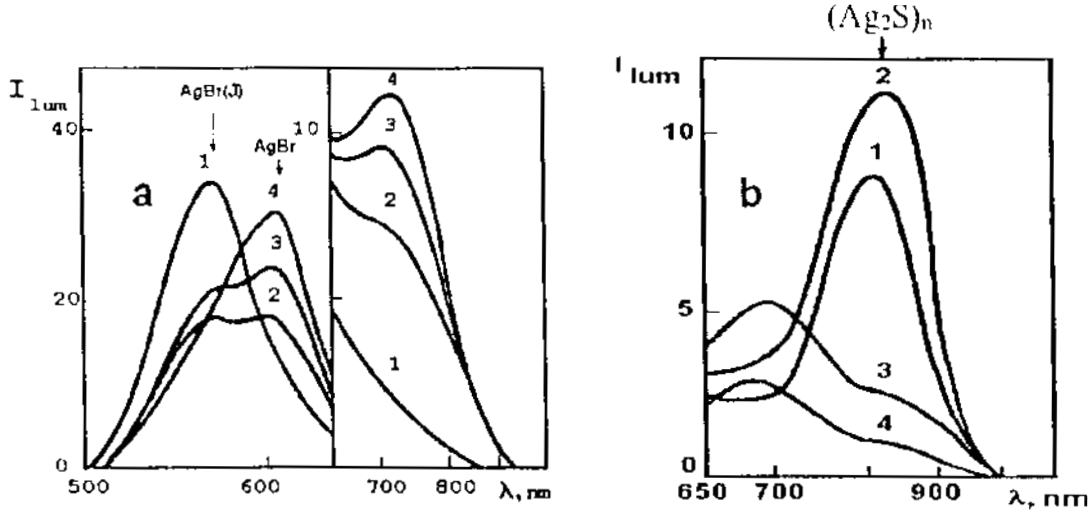

Figure 20. Photoluminescence spectra of sulfur-sensitized AgBr(I) microcrystals coated with AgBr shell with various thicknesses (≈): 1 — 0; 2 — 25; 3 — 100; 4 — 400. For excitation: (a) λ_{ex} = 400 nm; (b) λ_{ex} = 520 nm. Intensity values are in arbitrary units.

impurities in AgBr (l_{max} = 497 nm, T = 4.2 K) and leads to green PL associated with iodine pair centers.[21]

The observed effects may have the following explanations: Because of interaction of the sulfur sensitizer with silver halide, some positively charged surface silver ions are used for $(Ag_2S)_n$ and mixed $(Ag_2S)_pAg_m$ cluster formation, which leads to an increase in the number of structural defects in the subsurface region of emulsion microcrystals [Fig. 19(a)], so that the net concentration of surface Br_s^- and I_s^- anions increases [the neutral electrical charge of the microcrystal is guaranteed by the presence of the byproducts of sulfur sensitization; these products are not shown in Fig. 19(a)]. These anions lead to excitation bands with λ_{max} = 470 and 490 nm in the excitation spectra for the orange luminescence of AgBr. Thus, during the initial stages of sulfur sensitization, the responses h_{470} and h_{490} exhibit an increase. In addition, the increase in defect concentration in subsurface layers should promote surface anion migration and, therefore, I_s^- I_s^- center formation.[21] These centers yield a new green PL band in emulsion microcrystals. Surface Br_s, I_s^- centers and pair I_s^- Is^- centers are hole traps. Therefore, due to sulfur sensitization, hole-accepting centers of nonsilver sulfide origin can be observed [Fig. 19(b)]. Light absorption by Br_s^- and I_s^- at room temperature corresponds to the excitation maxima, λ_{max} = 470 and 490 nm, in the PL of sulfur-sensitized emulsions.[39] As t_2 increases, new centers—electron traps—are created. The capture of electrons by these centers results in the decrease of h_{470} and h_{490} [see Fig. 18(b), Curves 1', and 1''].

As was mentioned earlier, AgBr orange PL arises by radiative recombination in the $(Br_s^-I_s^0$ ..., $Ag^0_s)$ pair. Therefore, it is clear why, at the initial stages of sulfur sensitization when concentration of Brs^- and I_s^- ions increases, the intensity of orange PL of AgBr and AgBr(I) emulsions, when excited by light absorbed by AgBr (λ = 365 nm), also grows.[42]

If a silver bromide shell is grown on sulfur-sensitized AgHal microcrystals, luminescence intensity assigned to silver sulfide clusters decreases and the emission peak shifts to shorter wavelengths (Fig. 20).[43,44] These effects correspond to a decrease of cluster size, which can, in turn,

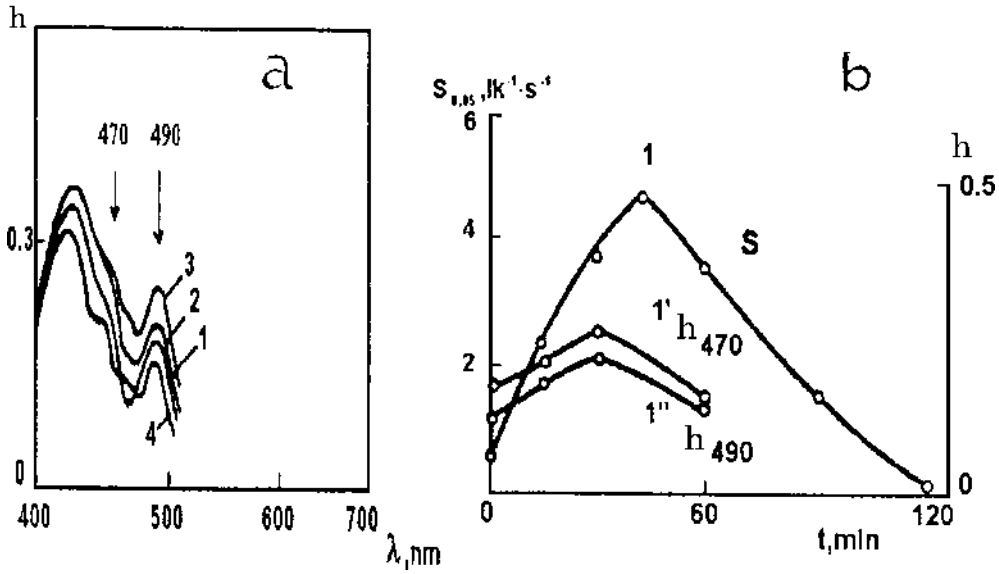

Figure 21. (a) Orange photoluminescence excitation spectra for samples of the reduction sensitized (2.47×10^{-4} mol thiourea dioxide/mol AgBr; pH = 6.0; pAg = 8.6; T = 47°C) 0.2-μm-cubic AgBr emulsion with various time periods (t_2, min) of digestion: 1 — t_2 = 0; 2 —15; 3 — 30; 4 — 60. Spectra are normalized at λ = 400 nm.
(b) Dependence of (1) photographic speed, (2) h_{470}, and (3) h_{490} on t_2. Values of h_{470} and h_{490} in arbitrary units.

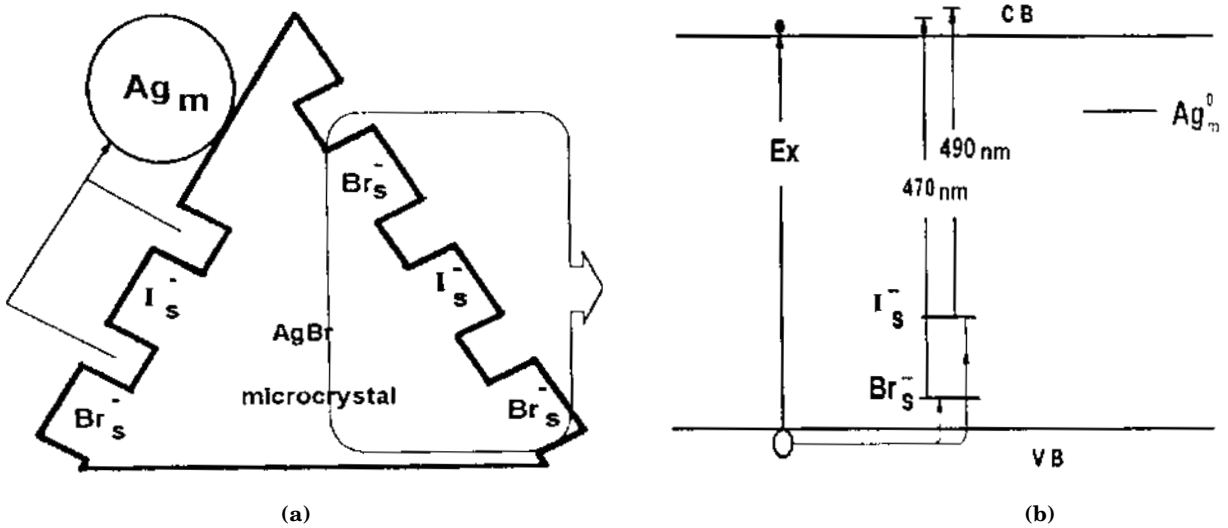

Figure 22. (a) Schematic diagram showing generation of silver clusters on the surface of reduction sensitized AgBr microcrystals by reaction of surface silver ions. (b) The energy levels of some impurity centers that appear in conjunction with reduction sensitization of AgBr emulsion grains.

be attributed to destruction (or dissolution) of the clusters during shell formation. This must be taken into account when one tries to understand the properties of emulsion with core–shell microcrystals.

Photoluminescence of Reduction-Sensitized Photographic Emulsions. In addition to sulfur sensitization we have conducted experiments on reduction sensitization using the following reducing agents: thiourea dioxide (I), diethanolamine (II), diethylamine (III), triethylamine (IV), triethanolamine (V), and β-diethylaminoethanol (VI). We have discovered that:

1. The peak intensity of low-temperature orange PL excited at 365 nm increases after adding reducing agents II - through VI into silver bromoiodide emulsions.[43]
2. Adding reducing agent I into silver bromide emulsions leads to an increase of h_{470} and h_{490} at the initial stages of reduction sensitization [Figs. 21(a) and (b)].[9]
3. Reduction sensitization decreases the intensity of PL determined by the adventitious iodine anion impurities in AgBr (l_{max} = 497 nm, T = 4.2 K) and leads to green PL of iodine pair centers.[21]

These results are similar to those obtained in the case of sulfur sensitization. Formation of silver clusters (Ag_m^0) during reduction sensitization involves silver ions from subsurface layers of the emulsion microcrystals [Fig. 22(a)]. This, again (see above) leads to increase of Br_s^- and I_s^- anion concentrations, and therefore the explanation previously presented for sulfur sensitization again can be applied.

Surface Br_s^-, I_s^- and $I_s^- I_s^-$ centers are hole traps, and, therefore, during reduction sensitization hole-accepting centers are created, but they do not necessarily comprise silver (Fig. 22).[20] It is very likely that these surface excess Br_s^- and I_s^- anions are R centers as proposed by Tani and Murofushi.[44] As shown above, the energy levels of these

anions lie between 0.24 and 0.51 eV above the top of the valence band of AgBr. Light absorption by these centers stimulates the PL bands with λ_{max} = 470 and 490 nm in the impurity sensitivity spectrum at room temperature.[9]

After hole localization on the surface Br_s^-, I_s^-, and $I_s^- I_s^-$ centers ($Br_s^- + h \Rightarrow Br_s^0$; $I_s^- + h \Rightarrow I_s^0$; $I_s^- I_s^- + h \Rightarrow I_s^- I_s^0$) its relocalization can follow the scheme:

$$\begin{aligned} (Br_s^0 ..., Ag_m^0) &\Rightarrow (Br_s^- ... Ag_m^+), \\ (Br_s^- I_s^0 ..., Ag_m^0) &\Rightarrow (Br_s^- I_s^- ..., Ag_m^+), \\ (I_s^- I_s^0 ... Ag_m^0) &\Rightarrow (I_s^- I_s^- ... Ag_m^+), \end{aligned} \qquad (25)$$

where Ag_m^0 is a essential part of the donor–acceptor pair (m = 2, 3, ...). The transformation of Ag_m^0 into Ag_m^+ according to Scheme 25 can be interpreted in terms of a hole-accepting function for silver centers of small size.[17] If the processes described by Sch. 25 occur at room temperature they should not lead to photoluminescence.

Conclusions

The results reviewed in this paper illustrate the great potential of the photoluminescence method to identify the nature and role of impurity centers created during chemical sensitization, as well as to suggest latent image formation mechanisms.

Acknowledgments. The author thanks Dr. A. Yu. Akhmerov, Dr. S. A. Zhukov, Dr. N. A. Orlovskaya, and Dr. O. I. Sviridova for their help in the accomplishment of the experimental investigations. He also wishes to thank Dr. M. R. V. Sahyun, University of Wisconsin, Department of Chemistry, Eau Claire, WI, for assistance in preparing the English manuscript. The author dedicates this paper to the memory of his teacher, Prof. K. V. Chibisov, whose 100th birthday will be celebrated on 1 March 1997.

References

1. M. Tsukakoshi and H. Kanzaki, *J. Phys. Soc. Japan* **30**: 1423 (1971).
2. V. M. Belous, V. I. Tolstobrov, V. P. Churashov, and V. V. Suvorin, *Zh. Nauch. i Prikl. Foto- i Kinematografii* **22**: 390 (1977).
3. V. M. Belous, *Zh. Nauch.i. Prikl. Foto-i Kinematografii* **12**: 297 (1967).
4. V. M. Belous, *Zh. Nauch. i. Prikl. Foto-i Kinematografii* **14**: 39 (1969).
5. F. Moser and F. Urbach, *Phys. Rev.* **106**: 852 (1957).
6. V. M. Belous and S. I. Golub, *Opt. i Spektroskop* **12**: 271 (1962).
7. V. M. Belous, *Zh. Nauch. i. Prikl. Foto-i Kinematografii* **35**: 304 (1990).
8. V. M. Belous, V. I. Tolstobrov, N. A. Orlovskaya, and S. A. Zhukov, *Izvestia AN SSSR, Seria Fizika* **45**: 272 (1981).
9. V. M. Belous, V. I. Tolstobrov, and K. V. Chibisov, *Dokl. AN SSSR*, **244**: 384 (1979).
10. V. M. Belous and V. I. Tolstobrov, *Zh. Nauch. i. Prikl. Foto-i Kinematografii* **27**: 66 (1982).
11. (a) V. M. Belous and N. G. Diachenko, *Opt. i Spektroskop* **10**: 649, (1961); (b) V. M. Belous, *Zh. Nauch. i. Prikl. Foto-i Kinematografii* **9**: 363 (1964).
12. V. M. Belous, N. G. Barda, E. A. Dolbinova, and Ch. B. Lushchik, *Zh. Nauch. i. Prikl. Foto-i Kinematografii* **23**: 460 (1978).
13. H. Kanzaki, *Photogr. Sci. Eng*, **24**: 219 (1980).
14. (a) M. S. Burberry and A. P. Marchetti, *Phys. Rev. B* **32**: 1192 (1985); (b) A. P. Marchetti and M. S. Burberry, *Phys. Rev. B* **28**: 2130 (1983).
15. W. Von der Osten and H. Stolz, *J. Phys. Chem. Sol.* **51**: 756 (1990).
16. V. M. Belous, A. L. Kartuzhansky, V. I. Matvienko, and L. I. Shur, (a) *Zh. Nauch. i. Prikl. Foto-i Kinematografii* **13**,157 (1968); (b) *Opt. i Spektroskop* **26**: 244, 740 (1969); **28**: 311 (1970).
17. V. M. Belous, S. A. Zhukov, E. A. Dolbinova, and A. Yu. Akhmerov, *Zh. Nauch. i. Prikl. Foto-i Kinematografii* **37**: 99 (1992)
18. J. W. Mitchell, *Usp. Fizi. Nauk* **67**: 293, 505 (1959).
19. A. Yu. Akhmerov and V. M.Belous, *Abstr. Symp. Photochemical and Photophysical Processes in Silver Halides,* Chernogolovka, p.46 (1991).
20. V. M. Belous, A.Yu. Akhmerov, S. A. Zhukov, N. A. Orlovskaya, and O. I. Sviridova, *Proc. 49th Annual Conference*, IS&T, Springfield, VA, 1996, p. 213.
21. V. M. Belous, *Uspechi Nauchnoi Fotografii* **25**: 5 (1989).
22. V. M. Belous, N. A. Orlovskaya, V. I. Tolstobrov, and K. V.Chibisov, *Dokl. AN SSSR* **235**: 1339 (1977).
23. V. M .Belous, V. I. Tolstobrov, V. P. Churashov, and K. V. Chibisov, *Dokl. AN SSSR* **236**: 645 (1977).
24. V. M. Belous, Yu. A. Breslav, V. I. Tolstobrov, and V. P. Churashov, *Zh. Nauch. i. Prikl. Foto-i Kinematografii* **22**: 452 (1977).
25. V. M. Belous and V. I. Tolstobrov, *Dokl. AN SSSR* **245**: 598 (1979).
26. V. M. Belous, V. I. Tolstobrov, K. V. Chibisov, and V. P.Churashov, *Zh. Nauch. i. Prikl. Foto-i Kinematografii* **23**:295 (1978).
27. C. T. Mumaw, *Photogr. Sci. Eng.* **24**: 77 (1980).
28. S. H. Ehrlich, *J. Imaging Sci. Technol.* **37**: 73 (1993).
29. V. M. Belous, V. I. Tolstobrov, O. I. Sviridova, and K. V. Chibisov, *Dokl. AN SSSR* **262**: 907 (1982).
30. E. Moisar, (a) *J. Photogr. Sci.* **14**: 181 (1966); (b) *Photogr. Sci. Eng.* **25**: 45 (1981).
31. M. K . Van Doorselaer, *J. Photogr. Sci.* **35**: 42 (1987).
32. D. A. Pitt, M. L. Rachu, and M. R. V. Sahyun, *Photogr. Sci. Eng.* **25**:57 (1981)
33. V. M. Belous, *Zhurnal Prikladnoi Spektroskopii* **62**: 42 (1995).
34. V. M. Belous, V. I. Tolstobrov, and K. V. Chibisov, *Dokl. AN SSSR* **246**; 632 (1979).
35. B. G. Ershov, G. V. Ionova, and A. A. Kiseleva, *Zhurn. Phys. Chemii* **69**: 260 (1995).
36. J. M. Hedges and J. W. Mitchell, (a) *Phil. Mag.* **44**: 357 (1953); J. H. Burrow and J. W. Mitchell, (b) *Phil. Mag.* **45**: 208 (1954).
37. K. V. Chibisov, *Chimia photograficheskoy emulsii* (Chemistry of photographic emulsions), *Nauka*, (1980) (in Russian).
38. P. Fayet, F. Granzer, G. Hegenbart, E. Moisar, B. Pischel, L. Wöste, *Phys. Rev. Lett.* **55**: 3002 (1985); Ch. Röshe, S. Wolf, T. Leisner, F. Granzer, and L. Wöste, *Proc. 47th Annual Conference*, IS&T, Springfield, VA, 1994, p. 54.
39. V. M. Belous, V. I. Tolstobrov, and K. V. Chibisov, *Dokl. AN SSSR* **244**: 628 (1979).
40. V. M. Belous and V.I. Tolstobrov, *Zh. Nauch. i. Prikl. Foto-i Kinematografii* **25**: 200 (1980).
41. V. M. Belous, V. I. Tolstobrov, O. I. Sviridova, and K. V. Chibisov, *Dokl. AN SSSR* **267**; 418 (1982).
42. V. M. Belous, L. P. Melnichuk, and K. V. Chibisov, (a) *Dokl. AN SSSR* **172**: 1357 (1967); (b) **175**: 349 (1967); (c) **182**: 862 (1968); (d) **193**: 1087 (1970).
43. V. M. Belous and V. I. Tolstobrov, *Zh. Nauch. i. Prikl. Foto-i Kinematografii* **25**: 299 (1980).
44. T. Tani and M. Murofushi, *J. Imag. Sci. Technol.* **38**: 1 (1994)
45. V. M. Belous, V. I. Tolstobrov, O. I. Sviridova, and K. V. Chibisov, *Dokl. AN SSSR* **264**: 1155 (1982).
46. V. M. Belous and A. L. Kartuzhansky, *Zh. Nauch. i. Prikl. Foto-i Kinematografii* **19**:114(1974).